*Acta Cryst.* (1987). B43, 326-333

# Structure Images and Superstructure Model of Calcic Plagioclase

BY A. KUMAO

*Department of Physics, Kyoto Institute of Technology, Sakyo-ku, Kyoto* 606, *Japan*

AND H.-U. NISSEN AND R. WESSICKEN

*Laboratorium für Festkörperphysik, Eidgenössische Technische Hochschule, CH-*8093 *Zürich, Switzerland*

(*Received* 1 *September* 1986; *accepted* 4 *March* 1987)

**Abstract**

Individual Ca and Na atom positions in the superstructure of low plagioclase with 67 mol% anorthite (An67) have been derived from high-resolution electron microscope images taken along different crystal axes. The Ca and Na occupancies are verified by comparing electron diffraction patterns with optical diffraction patterns obtained from masks representing the projected Ca and Na atom positions. A three-dimensional representation of the structure model is made on the basis of the arrangement of Ca/Na atoms. Lamellar anorthite-like domains occur along the periodic antiphase boundaries which are nearly parallel to the $(16\bar{7})$ plane. (This index refers to $c \simeq 14$ Å.) The lamellar domains sandwiched between the anorthite-like domains consist of a material in which the number of Ca and Na atoms is equal. Some of the electron microscope structure images are interpreted by comparison with ones calculated with a simplified version of the model.

## 1. Introduction

The intermediate plagioclase feldspars, the composition of which is in the range An25-An75, have a complicated superstructure associated with satellite reflections. Since this satellite problem was first studied by Chao & Taylor (1940), a number of different models analyzed by X-ray diffraction have been proposed. The first detailed interpretation of the satellite reflections of labradorite was made by Korekawa & Jagodzinski (1967), who introduced a density modulation of Ca/Na atoms. Subsequently, Korekawa's group extended this theory and carried out an analysis of the superstructure of feldspars (Korekawa & Horst, 1974; Jagodzinski & Korekawa, 1976, 1978; Korekawa, Horst & Tagai, 1978). The final result of the structure of a labradorite An52 was reported by Horst, Tagai, Korekawa & Jagodzinski (1981), in which a three-dimensional model of the superstructure was illustrated. Toman & Frueh (1976) also carried out a structure determination of an An55 by taking into account a shift modulation of the aluminosilicate framework. Kitamura & Morimoto (1977) proposed superstructure models of An25-An75 by assuming a shift modulation of Ca atoms and coexistence of anorthite-like and albite-like bands.

In view of the differences among the models proposed, high-resolution electron microscopy (HREM) has been applied to a specimen of An54 by Hashimoto, Kumao, Endoh, Nissen, Ono & Watanabe (1975). By interpreting the image contrast they suggested that the superstructure is due to the alternating arrangement of Ca and Na sites. Details of the refined model of an An50 were reported by Kumao, Hashimoto, Nissen & Endoh (1981). Similar images were published by Nakajima, Morimoto & Kitamura (1977), but the explanation of the image contrast was quite different from that given by Hashimoto *et al.* (1975). Tagai, Joswig, Korekawa & Wenk (1980) determined the occupational probabilities of Al and Si sites in An66 by means of neutron diffraction.

In this paper, Ca and Na positions in An67 are derived from HREM, and a superstructure model is proposed. The image contrast calculated will be discussed in comparison with the observed images.

## 2. Experimental

A specimen having 69 mol% anorthite (An69) from Sognefjord, Norway (Nissen, 1974) was selected for the electron microscope observation. The cell parameters of low plagioclases change with composition (Bambauer, Eberhard & Viswanathan, 1967); in accordance with this trend the following lattice constants were used throughout the present study:

$$a = 8{\cdot}17, \quad b = 12{\cdot}86, \quad c = 14{\cdot}22 \text{ Å};$$

$$\alpha = 93{\cdot}6, \quad \beta = 116{\cdot}2, \quad \gamma = 89{\cdot}8°.$$

Although the occupancies of individual atoms in plagioclase have not been discriminated, the sites of $M$(Ca/Na) atoms, $T$(Al/Si) atoms and O atoms have been proposed by several workers. In order to analyze the superstructure, we used the atomic coordinates for An55 given by Toman & Frueh (1973) for space group $C\bar{1}$ with a subcell $c \simeq 7$ Å and translations of $\mathbf{c}/2$, $(\mathbf{a}+\mathbf{b})/2$ and $(\mathbf{a}+\mathbf{b}+\mathbf{c})/2$ after Korekawa &

0108-7681/87/040326-08$01.50 

Table 1. *Coordinates of* Ca/Na *sites in the anorthite cell*

Indices in the left column refer to each atom.

| | $x$ | $y$ | $z$ |
|---|---|---|---|
| 1 | 0·2689 | 0·9767 | 0·0832 |
| 1′ | 0·7689 | 0·4767 | 0·5832 |
| 2 | 0·7305 | 0·9729 | 0·4463 |
| 2′ | 0·2305 | 0·4729 | 0·9463 |
| 3 | 0·7305 | 0·9729 | 0·9463 |
| 3′ | 0·2305 | 0·4729 | 0·4463 |
| 4 | 0·2689 | 0·9767 | 0·5832 |
| 4′ | 0·7689 | 0·4767 | 0·0832 |

Jagodzinski (1967). The atomic coordinates of Ca/Na were thus derived; these are the atoms which are most important in interpreting the superstructure of plagioclase. These Ca/Na coordinates are shown in Table 1, in which indices in the left column refer to each atom.

A small fragment of a specimen was crushed in pure alcohol with an agate mortar. Powdered crystals were dispersed on a copper grid covered with a holey carbon film and were observed by a JEM 200CX electron microscope operating at 200 kV, which was equipped with a ±10° top-entry tilting stage. High-resolution images taken in four orientations, *i.e.* along the three main axes [100], [010], [001] and [111], were computed by means of the multislice method using a simplified model not including any antiphase boundaries.

In order to check the Ca and Na positions in the superstructure of An67, two types of optical diffractograms were compared with electron diffraction patterns. One was made from small regions of the structure images taken in optimum focus condition. The other optical diffractograms were made with two-dimensional structure projection models in which Ca and Na atoms were represented by circular holes. Since the light scattering amplitude from a small hole of radius $a$ is proportional to $a^2$, the models of the structure projections were made in such a way that the ratio of the radii of holes representing Ca and Na was $\sqrt{2}:1$, because the atomic scattering amplitude of Ca is about twice that of Na for all scattering angles.

## 3. Interpretation of image contrast and diffraction pattern

Intermediate plagioclases near An67 commonly consist of heterogeneous exsolved structure units on a scale of several thousand ångström (Nissen, 1974). Owing to the small size of these lamellae it is difficult to examine critically the structure of each domain by means of X-ray diffraction. An example of heterogeneity is seen in the electron micrograph of Fig. 1(*a*), which was taken in [100] orientation. The center region of this figure is part of a very narrow exsolution lamella (about 500 Å thick) of an anorthite (An100). The optical diffraction pattern made from this area is shown in Fig. 1(*b*), in which only type *a* and *b* reflections are present. Type *b* reflections are characteristic of anorthite. In the right and left parts, broad fringes represent the antiphase domain structure of calcic plagioclase. The antiphase boundaries, however, are not clearly recognized. The reason for this fact is that the boundary plane $(16\bar{7})$, which will be determined from the next figure, is inclined about 10° to the incident electron beam. Fig. 1(*c*) shows the optical diffractogram made from the image of the right part, in which *a* reflections and *e* satellites occur. These satellites originate from the superstructure of plagioclase in the composition range An40–An75. Fig. 1(*d*) shows the electron diffraction pattern corresponding to the whole area shown in (*a*); the pattern consists of a superposition of the pattern of anorthite with that of calcic plagioclase. Note that the lattice planes at the anorthite/plagioclase phase boundary are not disturbed. This indicates complete coherence of the two structures.

Fig. 2(*a*) shows the electron micrograph of a specimen of An69 taken in the [111] orientation. The distance between the dark fringes is about 45 Å, corresponding to the distance between the satellite pairs in the diffraction pattern shown in the inset. The fringes are nearly parallel to $(16\bar{7})$, which plane is

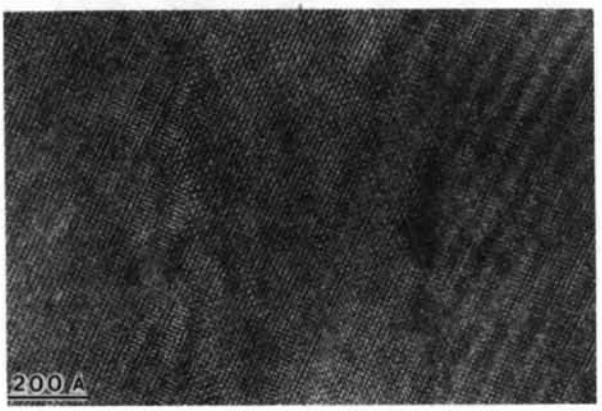


(*a*)


(*b*) (*c*) (*d*)

Fig. 1. (*a*) Electron micrograph taken along the *a* axis, showing the structural heterogeneity. (*b*) and (*c*) show the optical diffraction patterns made from the micrograph in the center and right areas, respectively. (*d*) Electron diffraction pattern corresponding to the whole area shown in (*a*).

normal to the plane of the micrograph. If this micrograph is looked at edge-on in the horizontal direction, it is found that rows consisting of white spots along the *a* direction in a bright fringe become grey in the adjacent bright fringes; the contrast of the white and grey rows is reversed in crossing the dark fringes. This contrast change is assumed to be caused by the periodic alternation of the sites of Ca and Na atoms as suggested by Hashimoto *et al.* (1975), who calculated the image contrast using a tentative model and showed that the positions of Ca atoms appeared darker than those of Na atoms in the optimum conditions. Fig. 2(*b*) shows the projected Ca/Na positions, in which the atoms contained within one unit cell are indicated by the same indices as given in Table 1. If a unit cell is shifted along any main axis in steps of one unit length, it can be found that atoms 1 and 1′, 2 and 2′, 3 and 3′, 4 and 4′ are superposed, respectively, and that four groups of atoms, 1–1′, 2–2′, 3–3′ and 4–4′ lie on parallel straight lines in the plane normal to [111] as shown in Fig. 2(*b*). A comparison of the image contrast with the projected atom positions suggests that atoms 1, 1′, 3 and 3′ correspond to Ca and atoms 2, 2′, 4 and 4′ to Na in a bright fringe, because atom rows 1–1′ and 3–3′ are close and appear as dark contrast, while atom rows 2–2′ and 4–4′ are also close and appear as lighter contrast in the optimum imaging condition as mentioned above. The Ca/Na arrangements are reversed in both adjacent bright fringes, *i.e.* atoms 1, 1′, 3 and 3′ correspond to Na and atoms 2, 2′, 4 and 4′ to Ca. The schematic illustration of the image is shown in Fig. 2(*c*), in which solid and dotted lines represent, respectively, the rows consisting of Ca atoms and of Na atoms. The ratio of the length of the solid and dotted line segments is 2:1, *i.e.* the total composition is An67. The narrow lamellae oriented parallel to $(16\bar{7})$, which are drawn only as solid lines, consist of a Ca-rich material with the anorthite (An100)-like structure. On the other hand, the bigger lamellae sandwiched between the narrow lamellae consist of a material in which the numbers of Ca and Na atoms are equal. This structure will hereafter be called the labradorite (An50)-like structure. In anorthite and albite, Al and Si sites are determined but they are not known with certainty in intermediate plagioclase. In the An50-like structure, therefore, we do not discriminate the occupancy of Al and Si atoms in this paper. The occupancy of Ca and Na atoms in the adjacent An50-like lamellae is in antiphase relation.

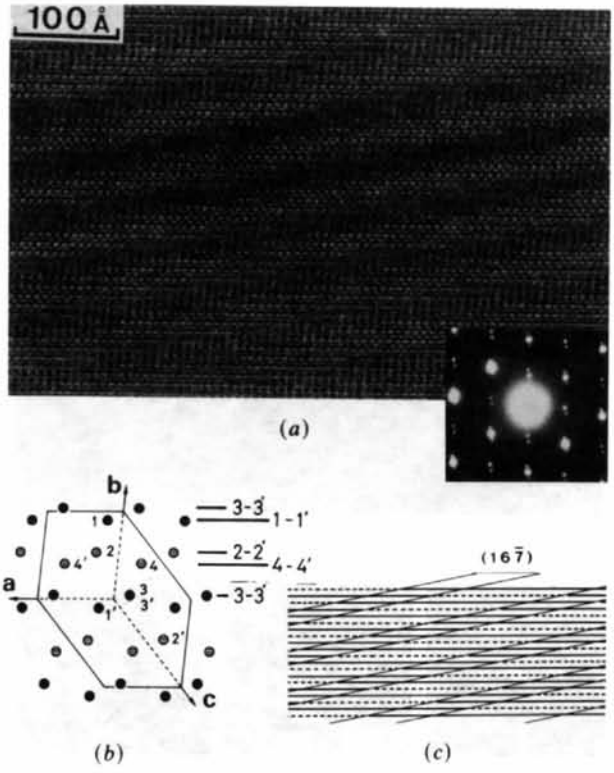


Fig. 2. (*a*) HREM image of a specimen of An69 taken along the [111] orientation together with the electron diffraction pattern. Dark fringes about 15 Å thick consist of anorthite-like structure. (*b*) Projected Ca/Na positions. Two kinds of atom groups are indicated as black and shaded discs. (*c*) Schematic illustration of the image in (*a*).

## 4. Three-dimensional structure model of An67

The contrast difference between lamellae having An50- and An100-like structures becomes clearest when the boundary is parallel to the electron beam. Therefore, if an index of the boundary and the thicknesses of the lamellae can be determined by considering carefully several micrographs and corresponding diffractograms taken along different crystal axes, a three-dimensional superstructure model of the plagioclase can be made. It is found in Fig. 2(*a*) that the thickness of the anorthite-like layers is about 15 Å; these layers comprise 10 unit cells along the *a* axis, while each labradorite-like lamella having about 30 Å thickness contains 20 unit cells along the *a* axis. As mentioned in the previous section, the occupancy of Ca and Na positions in the An50-like lamellae is reversed every 20 unit cells along the *a* axis when passing across the An100-like lamella.

Since the boundary plane of the lamella is $(16\bar{7})$, the origins of all unit cells located at $n(\mathbf{b}-6\mathbf{a})$, $n(\mathbf{c}+7\mathbf{a})$ and $n(7\mathbf{b}+6\mathbf{c})$, where $n$ is an integer including zero, are in the same plane parallel to $(16\bar{7})$. Moreover, the Ca and Na positions within those unit cells must have the same occupancy as in the unit cell at the origin, *i.e.* Ca and Na atom arrangements in each An50-like lamella placed between An100-like lamellae are identical. Fig. 3 shows the superstructure model of An67 constructed according to the rules outlined. In the white regions of the drawing, positions 1, 1′, 3 and 3′ are occupied by Ca, and 2, 2′, 4 and 4′ by Na. In the dotted regions, by contrast,

positions 1, 1′, 3 and 3′ are occupied by Na, and 2, 2′, 4 and 4′ by Ca. Thus the occupancy with regard to the Ca and Na positions is in antiphase relation in the white and dotted regions. In the black regions all cation positions, 1, 1′, 2, 2′, 3, 3′, 4 and 4′, are occupied by only Ca atoms, *i.e.* these regions have anorthite-like composition.

### 5. Image simulation and optical diffraction

Since the number of atoms contained within one superstructure unit is about $3\times10^4$, it is difficult to make a complete contrast calculation of the image with the computer equipment available at present. Therefore the images were computed by using a simplified model not including any boundary. Calculations were performed with the multislice method (Cowley & Moodie, 1957) by means of the program of Skarnulis (1979). Since it was found that there was little difference between images calculated using Al atoms only and images calculated using Si atoms only as $T$ atoms, the scattering amplitude of Al was adopted in the image simulations. The optical diffraction technique is another useful tool providing valuable information for analyzing the crystal structure in comparison with the electron diffraction patterns (Lipson & Michael, 1974). However, multislice programs reflect upon dynamical effects while optical diffraction relates to kinematical effects. Therefore, when we compare electron diffraction patterns with optical diffraction patterns, it must be emphasized that a crystal is extremely thin and images are taken under optimum focus condition. In the case of the thicker crystals studied in this paper, only positions of diffraction spots can be compared in the two different techniques. In this section we report the results of image simulation and optical diffraction carried out in order to check the proposed superstructure model of An67.

First, the results with regard to an anorthite (An100) crystal are represented so as to elucidate the difference in image contrast between An100 and An69. Fig. 4(*a*) shows the HREM image and the electron diffraction pattern of An100 observed along [010]. The inset figure shows the image calculated for a crystal of 77 Å thickness (six unit cells in the *b* direction) with the following parameters: accelerating voltage 200 kV, spherical aberration coefficient 1.2 mm, defocus value 600 Å, number of excited beams $N = 371$, while $n = 57$ is the number of beams which fall inside the aperture having a radius of $0{\cdot}6$ Å$^{-1}$ in reciprocal space. The positions of both large and small white spots in the image correspond to the tunnels surrounded by Ca and Al/Si atoms in the projected structure, which can be represented by replacing all Na atoms by Ca atoms in Fig. 5(*c*). Note that strong *a* reflections and weak *b* reflections are seen in the diffractogram. Fig. 4(*b*) shows the image of a specimen of An69 and the corresponding electron diffraction pattern in the same orientation as Fig. 4(*a*). The contrast pattern of the images in (*a*) and (*b*) is similar. This means that the crystallographic data of both specimens, An100 and An69, are almost the same. The difference between both images is that the small well separated bright spots in (*a*) are weak and continuous in (*b*). This is attributed to the existence of Na atoms in this specimen. The image

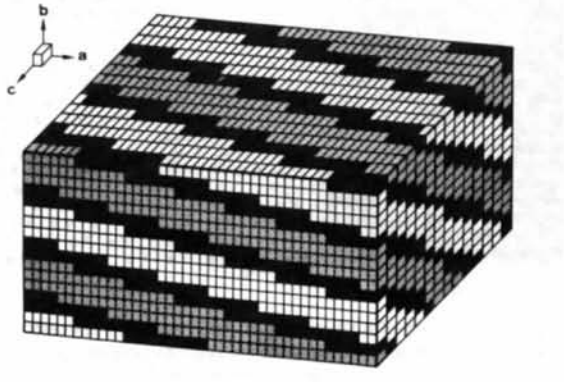


Fig. 3. Schematic drawing of the superstructure model of a plagioclase An67. Ca and Na atom arrangements in white and dotted regions are in antiphase relation. Black regions contain only Ca atoms. Boundary plane is $(16\bar{7})$.

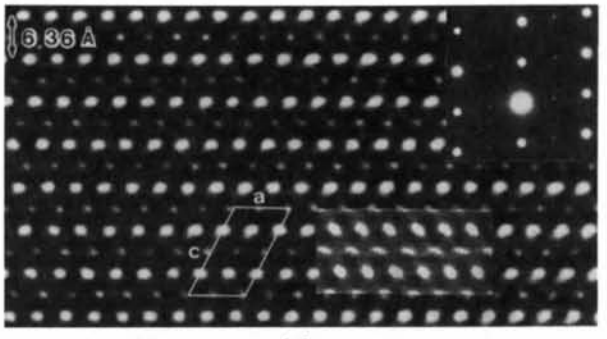


(*a*)

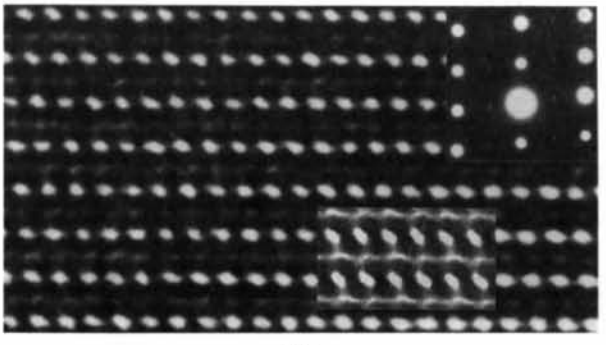

(*b*)

Fig. 4. Electron micrographs and diffractograms of the specimens, An100 (*a*) and An69 (*b*), taken in the [010] orientation. The computed images using the models of An100-like structure and An50-like structure are inserted in micrographs (*a*) and (*b*), respectively. The unit cell is indicated by white lines in (*a*).

inserted in (*b*) is an image computed using the model for the An50-like structure unit, which is drawn in Fig. 5(*c*) but with all O atoms omitted. Calculations were carried out with the same parameters as given above except for $N = 391$ and $n = 85$. Good agreement between the observed and computed images is obtained in (*b*) as well as in (*a*). It should be noted that in the real specimen of An69 the An100-like and An50-like structures are superimposed in the *b* direction because the domain boundaries are not parallel to the *b* axis as shown in Fig. 3. Therefore the ratio of the superpositions of Ca and Na atoms in the [010] projection depends on the positions and varies with the thickness of the specimen. However, it is reasonable to make a contrast calculation using the model of An50-like structure if the specimen is sufficiently thin. Note that very weak *e* satellites are seen in the electron diffraction pattern inserted in Fig. 4(*b*) instead of *b* reflections in (*a*). Fig. 5(*a*) shows the optical diffraction model of An67 constructed by plotting the Ca and Na positions in one layer in the [010] direction. In the figure the replacement of Ca and Na atoms near the domain boundaries was done as suggested in An50 by Kumao, Hashimoto, Nissen & Endoh (1981), but the effect of the replacement on the optical diffraction pattern was negligibly small. In Fig. 5(*a*) large and small discs represent Ca and Na atoms, respectively, where the radii of those discs are proportional to the square root of the atomic scattering amplitudes of Ca and Na atoms. The dotted lines indicate the boundaries between An100-like and An50-like structures. It is clearly seen that narrow layers sandwiched by dotted lines consist of An100-like structure. The optical diffractogram made from this model is shown in Fig. 5(*b*). It agrees with the electron diffractogram inserted in Fig. 4(*b*) with regard to the positions of *a* and *e* spots. Fig. 5(*c*) shows the Ca, Na and Al/Si positions in the An50-like structure in the [010] projection.

Fig. 6(*a*) is the image of an An69 taken along [111]. For this projection, since the periodic antiphase boundary ($16\bar{7}$) is perpendicular to the plane of the micrograph, two kinds of domains having respectively the An100-like and the An50-like structure can be recognized as a difference in image contrast. The regions indicated by thick arrows are darker than those indicated by thin arrows. Therefore the darker regions appear to correspond to the An100-like struc-

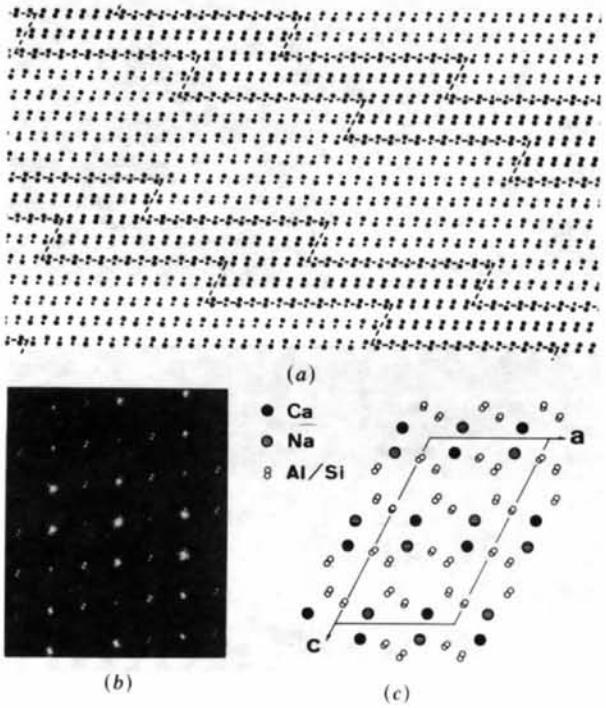


Fig. 5. (*a*) Optical diffraction model of An67, in which projected Ca/Na positions are drawn. (*b*) Optical diffraction pattern made from the model. (*c*) Projection of An50-like structure except for O atoms. If all Na atoms are replaced by Ca atoms, the structure becomes an An100-like structure.

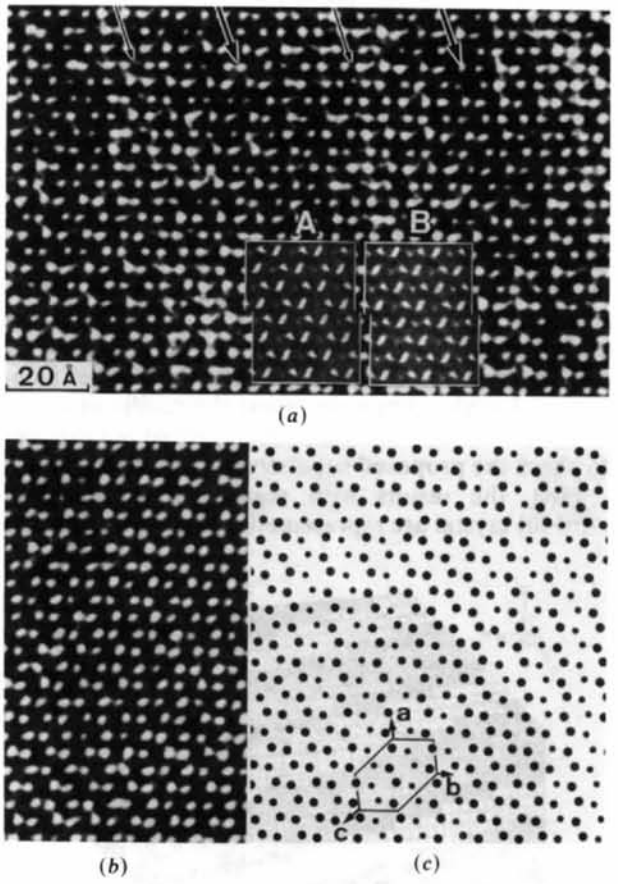


Fig. 6. (*a*) Image of a specimen of An69 in the [111] orientation. Thick and thin arrows indicate the regions consisting of An100-like and An50-like structures, respectively. The computed images corresponding to those structures are inserted as the insets *A* and *B*. Under-focus value is 750 Å. (*b*) Image of an anorthite (An100) in the same orientation. (*c*) A part of the optical diffraction model of An67 representing Ca and Na atom positions.

ture and the other regions to the An50-like structure, as suggested earlier. In order to explain the image contrast, calculations were made for a crystal of 88 Å thickness using the models with An100-like and An50-like structures, respectively. The results simulated with almost the same parameters for both structures are shown as insertions *A* and *B* in the micrograph. In *A*, which has an An100-like structure, the contrast of the center surrounded by six white spots is not very bright, while it is rather bright in *B*, with an An50-like structure. The difference is caused by the presence or absence of Na atoms in the two structures. Thus, as a whole, anorthite-like domains appear dark and labradorite-like domains appear bright in both the observed and the computed images. Therefore the image contrast could be interpreted sufficiently well, although the simplified model excluding antiphase boundaries in the unit cell was used in the simulations. An electron microscopic image of an anorthite (An100) taken from the same direction is given in Fig. 6(*b*) in order to compare with the contrast of An69. The contrast pattern of white spots appears uniform in the whole area of the micrograph. Fig. 6(*c*) shows a part of the optical diffraction model of An67 drawn on the same scale as that of the image. The model was made on the basis of the projected Ca/Na positions as shown in Fig. 7(*a*) and the superstructure model of Fig. 3. In Fig. 6(*c*) large discs represent the superposition of two Ca atoms, intermediate discs one Ca and one Na atom, and small discs two Na atoms. The sequence of superpositions of Ca and Na atoms in this projection is repeated when the thickness of the specimen increases. Fig. 7(*b*) shows the corresponding electron diffraction pattern. Figs. 7(*c*) and (*d*) are the optical diffraction patterns made from the image of Fig. 6(*a*) and the model of Fig. 6(*c*), respectively. Except for higher order *e* satellites in Fig. 7(*c*), these three patterns are nearly identical. This fact shows that the image of Fig. 6(*a*) has been taken under optimum focus conditions (Tanji & Hashimoto, 1978), and the proposed model is supported by this fact.

The next orientation to be discussed is a special case. Figs. 8(*a*) and (*b*) show the electron micrograph and the corresponding electron diffraction pattern of a specimen of An69 taken along [001]. In this projection, one Ca and one Na atom in a unit cell with the An50-like structure are always superposed as shown in Fig. 8(*c*), in which not only Ca/Na but also Al/Si atom positions are drawn and indices refer to Ca/Na atoms within a unit cell. Although unit cells with An50-like and others with An100-like structure are superimposed in the [001] direction, the difference of the bulk projected potential will be very small at any projected Ca/Na positions. Thus the contrast of the antiphase boundaries based on the Ca/Na arrangement does not appear in the micrograph and the satellite reflections are missing in the diffractogram. The calculated image using the An50-like structure is inserted into the micrograph on the right-hand side, since the contrast pattern of this image is almost the same as the image calculated with the

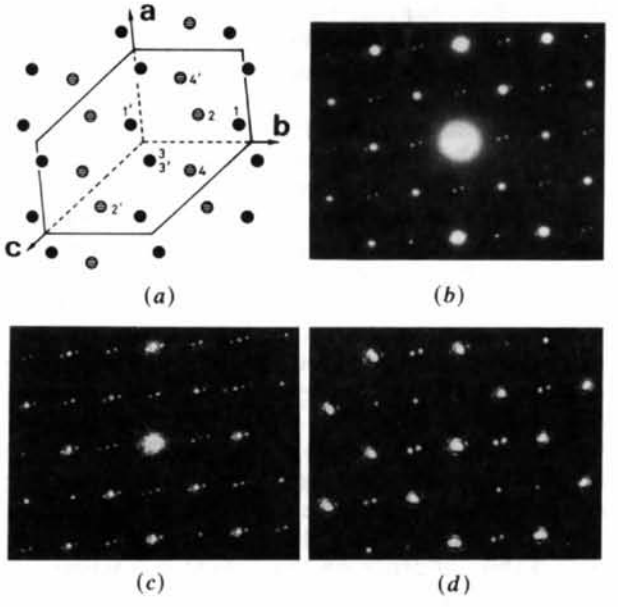


Fig. 7. (*a*) Projected Ca/Na atom positions along the [111]. (*b*) Electron diffractogram corresponding to the image of Fig. 6(*a*). (*c*), (*d*) Optical diffraction patterns made from the negative film of the image in Fig. 6(*a*) and the model in Fig. 6(*c*), respectively.

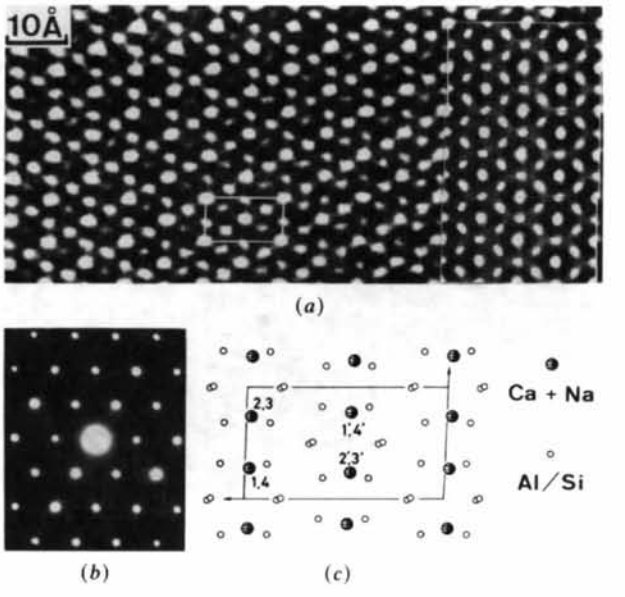


Fig. 8. (*a*) HREM image along [001], in which the image computed with An50-like structure is inset. The thickness of the specimen is 71 Å. Under-focus value 600 Å. (*b*) Electron diffraction pattern. (*c*) Projected Ca/Na and Al/Si atom positions, where one Ca and one Na are exactly superimposed in a unit cell of An50-like structure.

An100-like structure. Good correspondence has been obtained between the observed and computed images.

Last, the results on the [100] orientation will be shown. Fig. 9(*a*) gives the structure image of a thin part of an An69 specimen. Since the boundary is tilted against the incident electron beam, the contrast of the antiphase boundary is not clear in this projection although the tilting angle is small. Fig. 9(*b*) shows the projection of the An50-like structure in which oxygen atoms are omitted. It is found that double Ca or double Na atoms appear in the tunnels surrounded by Al/Si atoms. The image computed with the An50-like structure is inserted in Fig. 9(*a*), where the positions of white spots correspond to the positions of tunnels, and spots with relatively weak contrast correspond to the double Ca positions. In the observed image, however, some spots which are expected to be bright appear dark, as shown by thick arrows. Conversely, some spots which ought to have dark contrast appear bright; these are indicated by thin arrows. These contrast anomalies may be due to disorder in the Ca/Na atom arrangement or they may occur because of the electron beam damage to which the specimen is subject during observation.

## 6. Discussion

Since the complicated structure of intermediate low plagioclase was first reported by Chao & Taylor (1940), many structure models based on X-ray analysis have been proposed. However, they contradict each other. In this paper, the superstructure of An67 based on the occupancies of Ca and Na atoms has been studied by means of new methods, *i.e.* high-resolution electron microscopy and the optical diffraction technique.

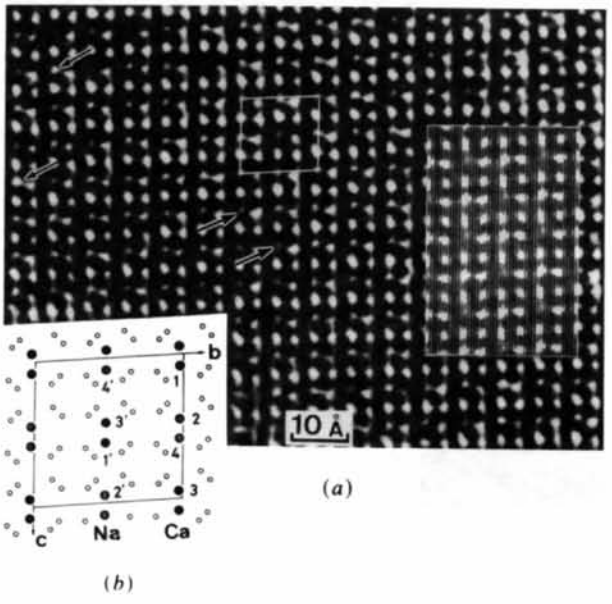


(*a*) (*b*)

Fig. 9. (*a*) Structure image taken along [100]. The inset is the image calculated with An50-like structure. The thickness of the specimen is 74 Å, under-focus value 500 Å. (*b*) Projected Ca, Na and Al/Si atom positions.

In an electron micrograph taken in the optimum imaging condition, the image contrast reflects the projected electric potential. Therefore, the alternation of darker and lighter contrast observed in the image along the [111] orientation reflects the preference of Ca and Na atoms rather than Al and Si atoms because the atomic scattering amplitude of Al is almost the same as Si while the amplitude of Ca is about twice that of Na over all scattering angles. This means that the superstructure of the plagioclase originates in a Ca/Na density modulation. Since it is difficult to determine the occupancies of Al and Si atoms from the structure images, these occupancies have not been considered in this paper. In order to check the superstructure model of An67 made on the basis of Ca/Na positions, the experimental images were compared with the ones calculated by using a model in which each unit cell has a simple structure, *i.e.* the An100-like and the An50-like structure, respectively. Although the boundary between An100-like and An50-like structures was not included in the calculations, we believe that a good fit between the observed and the computed images was obtained for four orientations. It is very important that the structure images taken from different directions could be interpreted without contradiction by the consistent use of the model made on the assumption of a Ca/Na density modulation.

Optical diffraction was used as a supplementary method for analyzing the superstructure of plagioclase. If a crystal is very thin and the structure image is taken under optimum focus conditions, the optical diffraction pattern made from the negative film is identical to the electron diffraction pattern. Moreover, so long as the structure model is possible in theory, the optical diffraction spots made from the two-dimensional structure projection model consisting of circular holes appear at the same positions as the electron diffraction spots. Because the optical diffraction pattern made from the projection model agrees with the electron diffraction pattern, the structure model is not always correct. However, it is a necessary condition for obtaining the right model. By comparing three kinds of diffraction patterns the occupancy of Ca/Na atoms in An67 was examined. The occupancy of Ca/Na atoms near the domain boundaries may not be systematic because the replacement of Ca or Na atoms near the boundaries did not result in any remarkable influence on the optical diffraction pattern as in the case of An50 (Kumao, Hashimoto, Nissen & Endoh, 1981). It should be emphasized that other optical models can produce optical diffraction patterns similar to the electron diffraction pattern, but the model proposed here is the only one which

does not contradict the structure image and the crystal structure given by Toman & Frueh (1973).

It is generally known that both the orientation and the spacing of satellites in X-ray and electron diffraction patterns vary with chemical composition of the plagioclase. The cause is attributable to the antiphase structure owing to the alternation of Ca/Na occupancy. For a specimen of An50, no Na-rich or Ca-rich regions exist (Kumao, Hashimoto, Nissen & Endoh, 1981). In a specimen of An67, it has been found that Ca-rich or anorthite-like regions exist along the antiphase boundaries in the form of thin layers. The thickness of the layers is assumed to increase with Ca content. For compositions containing less Ca than An50, Na-rich or albite-like regions may occur along the boundaries (Nissen, 1982). Thus, the superstructure of plagioclase feldspar probably consists of three basic structures, *i.e.* the albite-like, the labradorite-like and the anorthite-like structure.

The authors are indebted to Professor H. Hashimoto, Okayama University of Science, for valuable discussions and encouragement, and to Dr J. Ylä-Yääski for his help in the computation work. Part of this work was supported by the Swiss National Science Foundation.

### References

BAMBAUER, H. U., EBERHARD, E. & VISWANATHAN, K. (1967). *Schweiz. Mineral. Petrogr. Mitt.* 47, 351-364.

CHAO, S. H. & TAYLOR, W. H. (1940). *Proc. R. Soc. London Ser. A*, **176**, 76-87.

COWLEY, J. M. & MOODIE, A. F. (1957). *Acta Cryst.* **10**, 609-619.

HASHIMOTO, H., KUMAO, A., ENDOH, H., NISSEN, H.-U., ONO, A. & WATANABE, E. (1975). *Proceedings of the EMAG Conference, Bristol*, pp. 245-250.

HORST, W., TAGAI, T., KOREKAWA, M. & JAGODZINSKI, H. (1981). *Z. Kristallogr.* **157**, 233-250.

JAGODZINSKI, H. & KOREKAWA, M. (1976). *Z. Kristallogr.* **143**, 239-277.

JAGODZINSKI, H. & KOREKAWA, M. (1978). *Phys. Chem. Miner.* **3**, 69-72.

KITAMURA, M. & MORIMOTO, N. (1977). *Phys. Chem. Miner.* **1**, 199-212.

KOREKAWA, M. & HORST, W. (1974). *Fortschr. Mineral.* **52**, 37-40.

KOREKAWA, M., HORST, W. & TAGAI, T. (1978). *Phys. Chem. Miner.* **3**, 74-75.

KOREKAWA, M. & JAGODZINSKI, H. (1967). *Schweiz. Mineral. Petrogr. Mitt.* **47**, 269-278.

KUMAO, A., HASHIMOTO, H., NISSEN, H.-U. & ENDOH, H. (1981). *Acta Cryst.* A**37**, 229-238.

LIPSON, H. & MICHAEL, W. S. (1974). *J. Appl. Cryst.* **7**, 577-585.

NAKAJIMA, Y., MORIMOTO, N. & KITAMURA, M. (1977). *Phys. Chem. Miner.* **1**, 213-225.

NISSEN, H.-U. (1974). *The Feldspars*, edited by W. S. MACKENZIE & J. ZUSSMAN, pp. 491-521. Manchester Univ. Press.

NISSEN, H.-U. (1982). Report presented at the Autumn Meeting of Schweiz. Mineral. Petrog. Ses., Bern.

SKARNULIS, A. J. (1979). *J. Appl. Cryst.* **12**, 636-638.

TAGAI, T., JOSWIG, W., KOREKAWA, M. & WENK, H.-R. (1980). *Z. Kristallogr.* **151**, 77-89.

TANJI, T. & HASHIMOTO, H. (1978). *Acta Cryst.* A**34**, 453-459.

TOMAN, K. & FRUEH, A. J. (1973). *Z. Kristallogr.* **138**, 337-342.

TOMAN, K. & FRUEH, A. J. (1976). *Acta Cryst.* B**32**, 521-525, 526-538.

*Acta Cryst.* (1987). B**43**, 333-343

# The Electron Density Distribution in Calcium Metaborate, $Ca(BO_2)_2$

BY A. KIRFEL

*Mineralogisches Institut der Universität Bonn, Lehrstuhl für Mineralogie und Kristallographie, Poppelsdorfer Schloss, D-5300 Bonn 1, Federal Republic of Germany*

(*Received* 24 *August* 1986; *accepted* 16 *March* 1987)

## Abstract

The room-temperature electron density distribution in $Ca(BO_2)_2$ has been studied by X-ray diffraction experiments on two crystals, I and II, up to $s = (\sin\theta)/\lambda = 0{\cdot}80$ and $1{\cdot}16$ Å$^{-1}$, respectively. Conventional structure refinements yielded $wR = 0{\cdot}025/0{\cdot}021$ for 603/1577 observed reflections. Data set II was used for high-order refinements with varying cut-offs in order to assess positional and thermal parameters least biased by bonding effects and to estimate a 'best' scale factor. Rigid pseudoatom multipole expansions up to hexadecapoles resulted in final agreement factors $wR = 0{\cdot}0064/0{\cdot}0088$ which represent highly significant improvements of the fit with observations. Parameters derived from the multipole refinements of both data sets I and II were used to calculate dynamic and static deformation density distributions and deformation potential distributions in interesting sections of the structure. The choice of the resolution of the Fourier synthesis is shown to affect $\Delta\rho(\mathbf{r})$, especially around the nuclear positions. The observed charge distributions are discussed in terms of chemical bonding in $Ca(BO_2)_2$ and in comparison with an earlier study on $LiBO_2$. In addition, spherical-charge integrations around Ca and B served to establish formal ionic radii and charges of the cations. All relevant results indicate a predominantly ionic interaction between $Ca^{2+}$ and the $(BO_2)^-$ anions (of metaboric acid) which polymerize to endless chains of

0108-7681/87/040333-11$01.50 